A multifractal analysis for electronic transmittance in inhomogeneous potentials

1992 J. Phys.: Condens. Matter 4 6095

(http://iopscience.iop.org/0953-8984/4/28/010)

J. Phys.: Condens. Matter 4 (1992) 6095–6107. Printed in the UK

A multifractal analysis for electronic transmittance in inhomogeneous potentials

Prabhat K Thakur†, Chaitali Basu‡, Abhijit Mookerjee‡ and Asok K Sen†

† Saha Institute of Nuclear Physics, AF 1 Sector I, Salt Lake, Calcutta 700064, India
‡ S N Bose National Centre for Basic Sciences, DB 17 Sector I, Salt Lake, Calcutta 700064, India

Received 25 June 1991, in final form 29 January 1992

Abstract. Electronic transmittance in a one-dimensional tight-binding incommensurate potential has been studied numerically for states in the vicinity of the mobility edge by multifractal analysis. Multifractal analysis shows a spectrum of scaling exponents for the normalized transmittance (over the system size) near the transition from extended to localized states. For the critical states we have computed dimensionless resistance related through the Landauer formula and shown that it does not have an exponential nature.

1. Introduction

Electronic states in incommensurate potentials exhibit some novel features that are distinct compared with those for periodic and random potentials. Several investigations have been carried out for a one-dimensional tight-binding model (Harper 1955, Aubry and Andre 1980, Kohmoto 1983, Ostlund and Pandit 1984, Basu *et al* 1991a):

$$\Psi_{n+1} + \Psi_{n-1} + V_n(Q)\Psi_n = E\Psi_n \tag{1}$$

where $|\Psi_n|^2$ is the local probability amplitude, $V_n(Q)$ is the site diagonal potential with Q being an irrational number and E is the energy. For various forms of $V_n(Q)$, the properties of the wavefunctions, their phases, the energy spectra and electronic transport have been studied so far mostly by numerical techniques (Kohmoto 1983, Ostlund and Pandit 1984, Basu *et al* 1991a).

The model defined by $V_n(Q) = \lambda \cos(2\pi nQ)$, which is known as the Harper model (Harper 1955, Aubry and Andre 1980), undergoes a metal–insulator transition such that the states for $\lambda < 2$ are extended, those for $\lambda > 2$ are localized and the state at $\lambda = 2$ becomes critical. Standard techniques like evaluation of Lyapunov exponents or the participation ratio do not seem to be appropriate for the characterization of the novel features present in the critical state. These have also been found in the Fibonacci model potential in one dimension.

In recent years a multifractal analysis for the characterization of such states in various quasi-periodic model potentials has been proposed. This clearly distinguishes the critical state (its energy spectra, integrated density of states, probability amplitudes) from extended or localized states (Aubry and Andre 1980, Kohmoto *et al* 1983, Kohmoto

1983). A class of more general model potentials has also been introduced, which exhibits an energy-dependent transition (mobility edge) in one-dimensional systems (Soukoulis and Economou 1982, Hiramoto and Kohmoto 1989, Das Sarma *et al* 1990). These potentials are deterministic and yet different in their behaviour from random potentials in the sense that, in one dimension, all eigenfunctions are not localized. Instead there appear metal–insulator transitions separating extended and localized states. The potential $V_n(\gamma, Q) = \lambda \cos(2\pi n^\gamma Q)$ having an inhomogeneous period $Qn^{\gamma-1}$ has been of much interest in recent years (Griniasty and Fishman 1988, Thouless 1988, Das Sarma *et al* 1990, Basu *et al* 1991a). It exhibits the following properties.

(i) It has mobility edges for $0 < \gamma < 1, 2 > \lambda$ (Das Sarma *et al* 1990, Basu *et al* 1991a).

(ii) All states (except states at the band centre) for $1 < \gamma < 2$ are localized. But the nature of the localized state at the band centre is different in the sense that the Lyapunov exponent vanishes very slowly there, as discussed by Thouless (Hiramoto and Kohmoto 1989). Localization in this system is different from purely exponential localization as in random chains.

(iii) Exponential localization as in a random system is shown by perturbative calculation for $\gamma \geq 2$ (Griniasty and Fishman 1988).

Recently Das Sarma *et al* (1990) have calculated the wavefunction, electronic density of states and Lyapunov exponent for the above model in the regime $0 < \gamma < 1$, which shows an energy-dependent transition at $E = (2 - \lambda)$. We have studied electronic transmittance and the phase of the outgoing electron for the above model potential in different energy regimes, with special emphasis on stages near the mobility edge (Basu *et al* 1991a). Fractal aspects for the spatial extension of the wavefunction have also been discussed before for one-dimensional disordered systems (Soukoulis and Economou 1989, Roman and Wiecko 1986). The model potential $V_n(\gamma, Q) = \lambda \cos(2\pi n^\gamma Q)$ for $0 < \gamma < 1$ is interesting in the sense that it has a gapless spectrum with a mobility edge even in one dimension. We have used the transfer-matrix method to study the transmittance for an electron through chains (of sizes $\sim 10^5$) with such a potential and attached in perfectly conducting leads or wires at both ends. The transmittance at the far end of the chain carries information of the effective scattering due to the incommensurate potential through the scattering matrix, which connects the solution on the two conducting sides of the chain.

In a series of earlier works (Aoki 1983, 1986, Schreiber 1985a, b, 1990, Kramer *et al* 1988, Ono *et al* 1989) it was asserted that the wavefunctions in random potentials were fractals. However, since they had studied the inverse participation ratio *alone*, their analysis could not probe the multifractal nature of these objects. In a recent communication Schreiber and Grussbach (1991) have carried out a multifractal analysis of *one* critical wavefunction in a three-dimensional random potential and one localized wavefunction in a one-dimensional random chain, for a *single* system size each. They have concluded that both the critical and the localized states are multifractal and comment 'it will therefore be an interesting problem to investigate whether the metal–insulator transition can be identified from such an analysis *in some way*'. In an earlier work on Azbel resonances (Basu *et al* 1991a) we have shown that the behaviour of the $f(\alpha)$ versus α curves as functions of system size clearly distinguishes between extended, localized and resonant states. Further, this analysis does not depend on individual states, but is a common feature of all similar states. In this communication we suggest this procedure to be a sensitive test to differentiate between extended, critical and localized states.

2. Formalism

2.1. Transfer-matrix method

Equation (1) can be written alternatively in terms of a transfer matrix at the site n as

$$M_n(\gamma, Q)\theta_n = \theta_{n+1} \tag{2}$$

$$M_n(\gamma, Q) = \begin{pmatrix} E - V_n(\gamma, Q) & -1 \\ 1 & 0 \end{pmatrix} \qquad \theta_n = \begin{pmatrix} \psi_n \\ \psi_{n-1} \end{pmatrix} \tag{3}$$

and $V_n(\gamma, Q) = \lambda \cos(2\pi n^{\gamma} Q)$ where Q is an irrational number for our work chosen to be $(\sqrt{5} - 1)/2$. The wavefunction amplitudes at the sites $N - 1$ and N are related to the initial points 0 and 1 through the following relation:

$$\begin{pmatrix} \psi_N \\ \psi_{N-1} \end{pmatrix} = P_{\gamma}^{N}(Q, E) \begin{pmatrix} \psi_1 \\ \psi_0 \end{pmatrix} \tag{4}$$

where $P_{\gamma}^{N}(Q, E) = M_N M_{N-1} \ldots M_3 M_2 M_1$. This follows directly from (2) and (3).

Now, solutions for regions $-\infty < n < 1$ and $N < n < \infty$ are of the following forms respectively:

$$\psi_n(-\infty < n < 1) = A \exp(ikn) + B \exp(-ikn) \tag{5a}$$

$$\psi_n(N < n < \infty) = C \exp(ikn) + D \exp(-ikn). \tag{5b}$$

The transfer matrix is defined so as to relate the amplitudes of the solutions of the Schrödinger equation in the perfectly conducting leads on either side of the chain of incommensurate potential $V_n(\gamma, Q)$. If there is an incident wave on the left, one can write for the right end of the conducting wire

$$\begin{pmatrix} \psi_{N+1} \\ \psi_{N+2} \end{pmatrix} = S\theta^{-1} \begin{pmatrix} D \\ C \end{pmatrix}$$

where

$$S = \begin{pmatrix} \exp(-ik) & \exp(ik) \\ 1 & 1 \end{pmatrix}$$

$$\theta^{-1} = \begin{pmatrix} \exp[-ik(N+1)] & 0 \\ 0 & \exp[ik(N+1)] \end{pmatrix}. \tag{6}$$

Now we define the scattering matrix T_N by

$$\begin{pmatrix} D \\ C \end{pmatrix} = T_N \begin{pmatrix} B \\ A \end{pmatrix}. \tag{7}$$

Similarly for the left end of the chain,

$$\begin{pmatrix} \psi_1 \\ \psi_0 \end{pmatrix} = S \begin{pmatrix} B \\ A \end{pmatrix}. \tag{8}$$

From equation (6), we have

$$S\theta^{-1}\begin{pmatrix} D \\ C \end{pmatrix} = P_\gamma^N(Q, E)S\begin{pmatrix} B \\ A \end{pmatrix}$$

$$\begin{pmatrix} D \\ C \end{pmatrix} = \theta S^{-1}P_\gamma^N(Q, E)S\begin{pmatrix} B \\ A \end{pmatrix} = T_N\begin{pmatrix} B \\ A \end{pmatrix}$$

where $T_N = \theta S^{-1}P_\gamma^N(Q, E)S$. Substituting into equation (4)

$$\begin{pmatrix} \psi_{N+1} \\ \psi_N \end{pmatrix} = \prod_{i=1}^{N} M^i \begin{pmatrix} \psi_1 \\ \psi_0 \end{pmatrix}. \tag{9}$$

From equations (5)–(9) and the definitions of reflectance and transmittance we obtain

$$\begin{aligned} &\text{reflectance} = |B/A|^2 = |T_N^{12}/T_N^{11}|^2 \\ &\bullet\ \text{transmittance} = (1 - |B/A|^2) = (1 - |T_N^{12}/T_N^{11}|^2). \end{aligned} \tag{10}$$

Therefore resistance from the Landauer formula can be written as

$$R(E, N) = \text{reflectance/transmittance} = |T_N^{12}/T_N^{11}|^2/(1 - |T_N^{12}/T_N^{11}|^2).$$

2.2. Multifractal analysis

Multifractal analysis is an adequate tool to look at singular behaviour of a normalized measure. We shall begin by considering a partition of the support [0, 1] into N intervals and defining a measure P_i in terms of the normalized transmittance as

$$P_i = T_i(E) \Big/ \sum_{i=1}^{N} T_i(E).$$

From the definition of transmittance $P_i \geqslant 0$ and $\Sigma^N P_i = 1$. We next define a partition function for any real number q and the given probability measure P_i in the ith subdivision (box) of the support in terms of the qth moment $\chi(q) = P_i^q$,

$$Z(q) = \sum_{i=1}^{N} \chi(q). \tag{11}$$

The measure is said to be multifractal whenever one has the scaling behaviour $Z(q) \sim N^{-\tau(q)}$, $P_i \sim N^{-\alpha}$.

The definition of the exponent $\tau(q)$ is related to the general dimension D_q in the following way:

$$\tau(q) = (q - 1)D_q. \tag{12}$$

Now, the number of boxes which cover the measure having exponents between α and $\alpha + d\alpha$ obeys a scaling behaviour $N_\alpha \sim N^{f(\alpha)}$.

One can write $Z(q)$ as an integral over the exponent α,

$$Z(q) \sim \int d\alpha\, N^{-[\alpha Q - f(\alpha)]}. \tag{13}$$

The dominant contribution in the integrand in (13) comes from the exponents that are

stationary with respect to α, i.e. for $q = (df/d\alpha)$. Thus, $\tau(q) = \alpha q - f(\alpha)$ and $\alpha = (d\tau/dq)$, since $f(\alpha)$ is independent of q, by definition.

Barabási *et al* (1991) have discussed the multifractal spectra of multi-affine functions. They have generalized the above analysis to note that, for multi-affine functions, a class to which the transmittance belongs, the multifractal spectra depend upon the partition used. Our analysis corresponds to their partition characterized by $\varphi = 1$.

The problem essentially boils down to getting α, the scaling exponent for the measure, and $f(\alpha)$ for the number of boxes that cover this measure. Thus the weight $f(\alpha)$ as a function of the scaling exponent α of the measure gives a spectrum of scaling exponents and fractal-like dimensions. The numerical technique for computing α and $f(\alpha)$ has been discussed in the literature (Halsey *et al* 1986, Basu *et al* 1991b). It is known that for the extended case α_{min} and α_{max} will converge towards 1 as the system size is increased; $f(\alpha_{min})$ and $f(\alpha_{max})$ also behave likewise converging towards 1. So for a large system we expect that for extended states the $f(\alpha)$ versus α curve would shrink to a point (1, 1). For a localized state, with increasing system size α_{min} should tend to 0. This corresponds to a large probability (ideally = 1) of getting the electron within the localization length. At the same time, α_{max} diverges, implying exponential decay of probability for lengths much larger than the localization length. A critical state, being intermediate between extended and localized states, is expected to show some intermediate behaviour with respect to scaling exponents also.

3. Results and discussion

We have carried out numerical calculations for the transmittance in the vicinity of the mobility edge for the above model to check the nature of states undergoing the metal–insulator transition. We have fixed the value of λ to 1 and have studied the behaviour of the transition from metal to insulator. The mobility edge has been predicted by Das Sarma *et al* (through heuristic arguments) to be at $E_c = \pm (2 - \lambda)$. But numerical calculation of inverse localization length (Sutherland and Kohmoto 1987) and transmittance versus energy (Basu *et al* 1991a) does not show a sharp mobility edge. We have shown the variation of transmittance (in figure 1) from ~1 (for $E < E_c$) to ~0 (for $E > E_c$). The energy E_c is chosen to be that point at which the transmittance is significantly different from 1 and 0.

We analysed the character of transmittance for $\gamma = 0.1$, 0.3 and 0.4 in the vicinity of E_c as a function of system size. In figure 1(*a*) for $\gamma = 0.1$, we have chosen the energy $E_c = 1$, and it is seen that the transition is fairly sharp. Figure 1(*b*) shows the same for $\gamma = 0.3$, and the energy is chosen to be 0.9945. Figure 1(*c*) shows the same for $\gamma = 0.4$, and here the energy is chosen to be 0.982.

In figure 2, transmittance is studied as a function of the system size at the above energies. As seen, there is an indication of a self-similar nature. Figures 2(*a*), (*b*) and (*c*) show that the transmittance versus system size for $\gamma = 0.3$ and 0.4 are similar to one another but they differ considerably from that for $\gamma = 0.1$ at this length scale.

The states for $E < E_c$ and $E > E_c$ show distinct physical nature for the transmittance as a function of system size through a scaling relation $N^{-\alpha}$. We studied the multifractal dimension $f(\alpha)$ versus scaling exponent α for the extended and critical states. Figure 3(*a*) shows $f(\alpha)$ versus α for systems of length 3×10^4 (———), 2×10^4 (– · – · –) and 10^4 (– – – –) taking all the moments q between −30 and +30 into consideration for a pure extended state with $\gamma = 0.0$. All three curves fall on one another. As seen, the peak

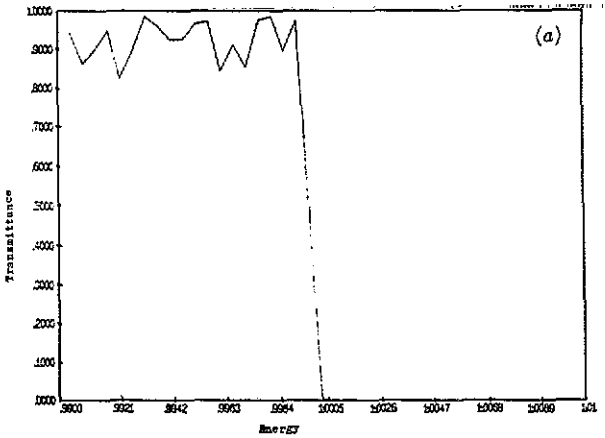

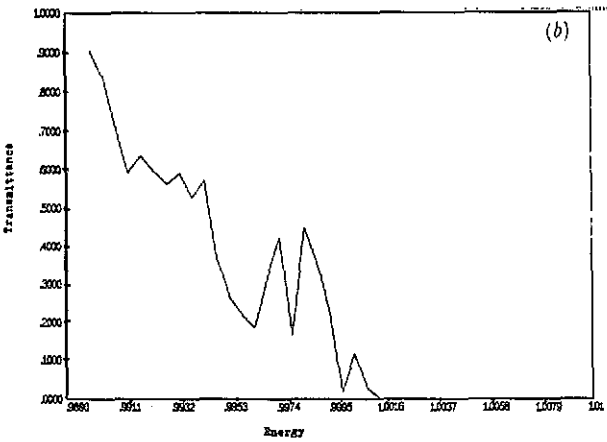

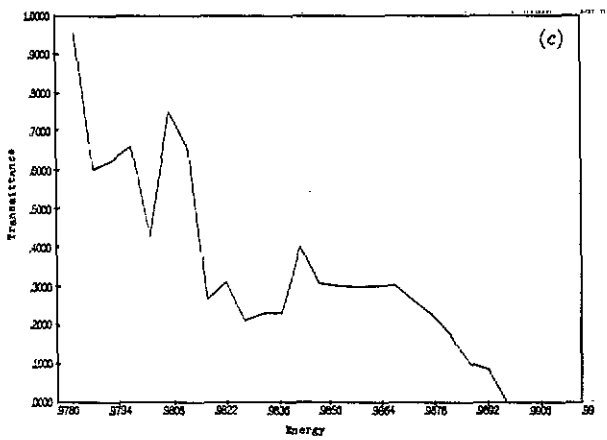

Figure 1. Transmittance versus energy for $\lambda = 1$ and system size 10^4: (*a*) $\gamma = 0.1$; (*b*) $\gamma = 0.3$; and (*c*) $\gamma = 0.4$.

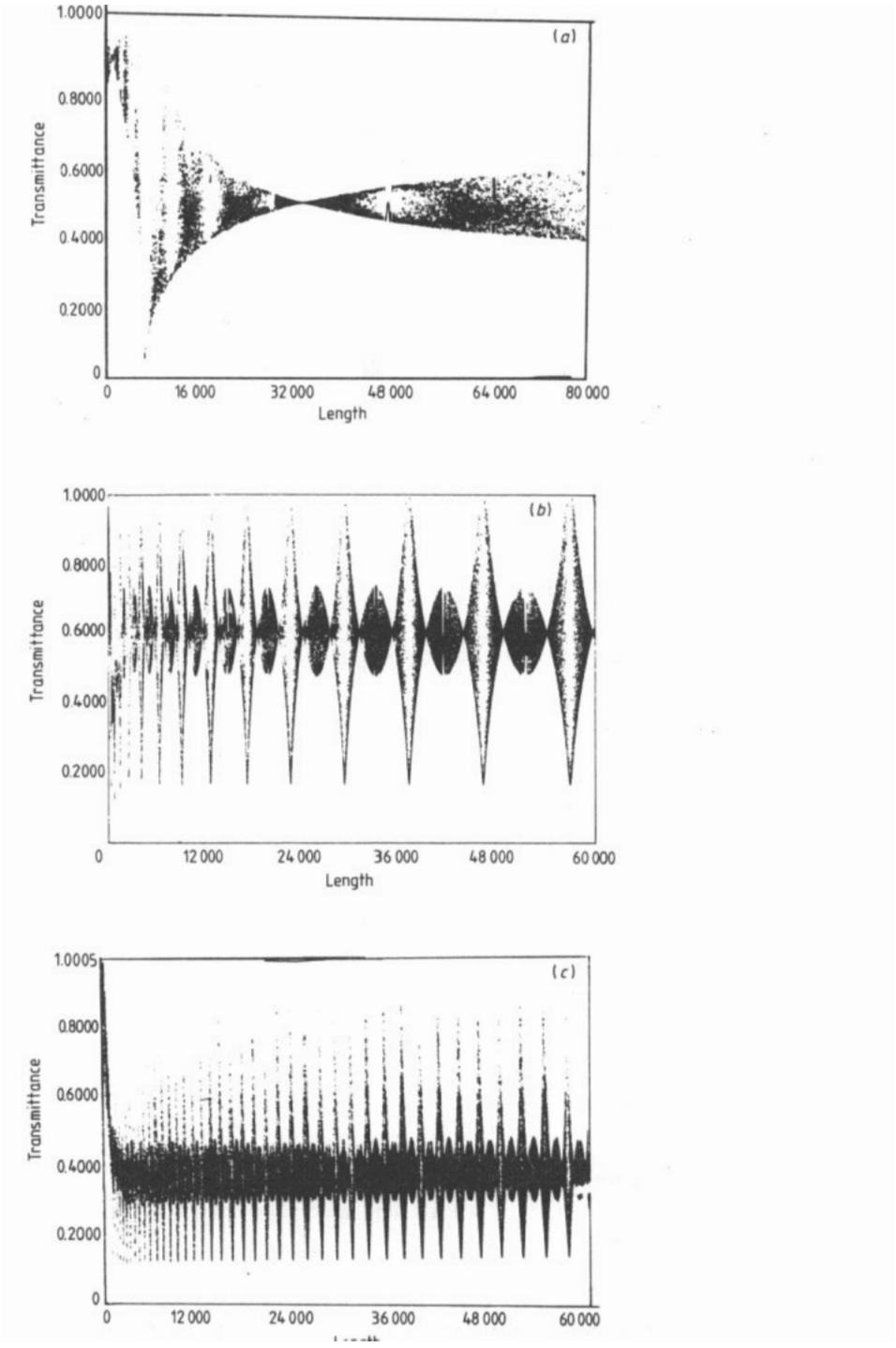

Figure 2. Transmittance versus length for: (*a*) $\gamma = 0.1$ for $E = 1.0$; (*b*) $\gamma = 0.3$ for $E = 0.9945$; and (*c*) $\gamma = 0.4$ for $E = 0.982$.

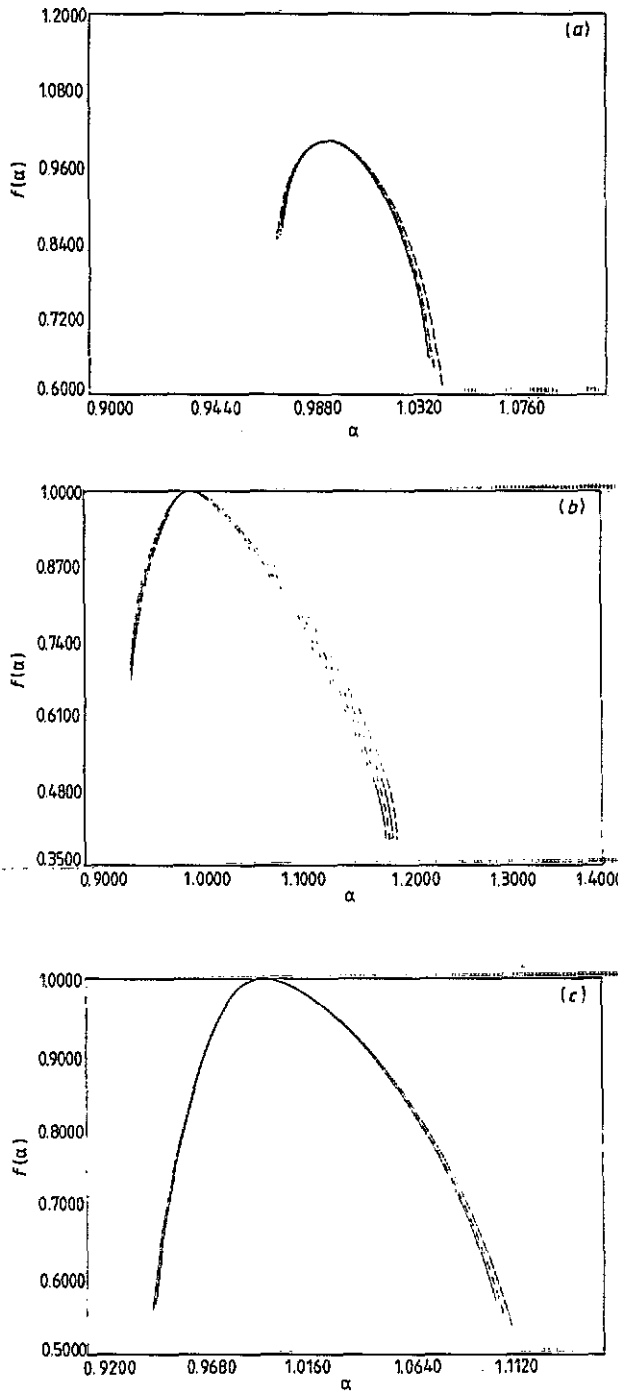

Figure 3. Plots of $f(\alpha)$ versus α for: (*a*) an extended state ($\gamma = 0.0$) for three system sizes 8000, 9000 and 10 000, $E = 0.0$; (*b*) a critical state with $\gamma = 0.1$ for system sizes 50 000, 60 000, 70 000 and 80 000, $E = 1.0$; and (*c*) a critical state with $\gamma = 0.3$ for system sizes 40 000, 50 000 and 60 000, $E = 0.9945$. (Energies of (*a*)–(*c*) are the same as those of figures 2(*a*)–(*c*) respectively.) See text for details of curves.

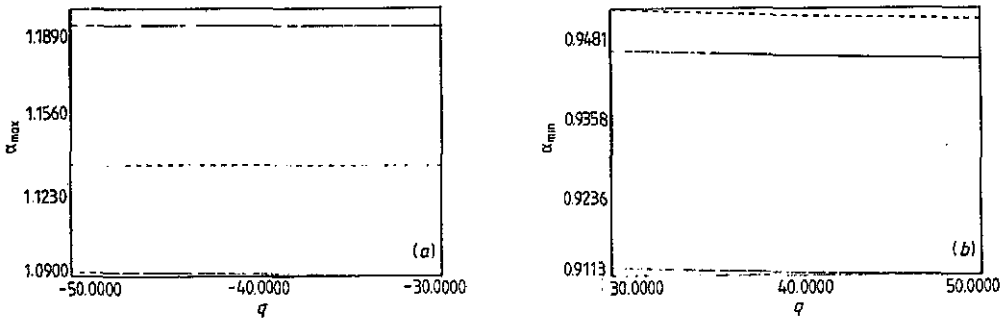

Figure 4. Plots of (*a*) α_{max} and (*b*) α_{min} versus q for $\gamma = 0.1$ (– – – –), $\gamma = 0.3$ (———) and $\gamma = 0.4$ (– · – · –).

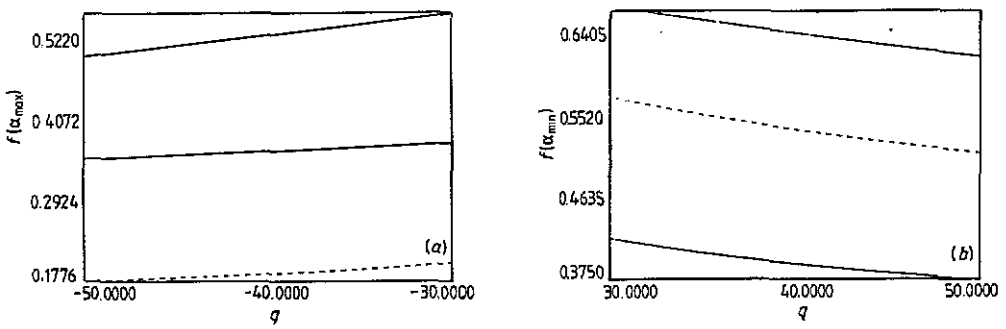

Figure 5. Plots of (*a*) $f(\alpha_{max})$ and (*b*) $f(\alpha_{min})$ versus q for $\gamma = 0.1$ (– – – –), $\gamma = 0.3$ (———) and $\gamma = 0.4$ (– · – · –).

is at $\alpha = f(\alpha) = 1$ and as expected the curve tends to collapse around this point with increasing length. The values of $f(\alpha_{min})$ at sizes 10^4, 2×10^4 and 3×10^4 are 0.8464, 0.8583 and 0.8643.

Figure 3(*b*) shows the same for $\gamma = 0.1$. The system sizes are 80 000 (———), 70 000 (– – – –), 60 000 (– · – · –) and 50 000 (— — — —). The state for $\gamma = 0.1$ has a very long quasi-period. Within our numerical limitation it is not possible to carry out the multifractal analysis fully for this γ. The essential feature of this figure is that, with increased system size, $f(\alpha)$ versus α curves shift inwards as in the extended state, but unlike the latter, $f(\alpha_{min})$ decreases with increasing size. Also the curves tend to converge on the α_{min} side. Figure 3(*c*) shows $f(\alpha)$ versus α curves for $\gamma = 0.3$. Here the multifractal nature of the state resembles critical states. Curves for three system sizes 60 000 (– · – · –), 50 000 (———) and 40 000 (– – – –) are drawn. There is no shift in a particular direction. The curves seem to oscillate and with increase in system size $f(\alpha_{min})$ and $f(\alpha_{max})$ both show a tendency to fall. This is a typical character of critical states.

Figure 4 shows the behaviour of α_{max} and α_{min} with increase in the order of the moments for a fixed system size for the three different γ values. Figure 4(*a*) shows α_{max} versus q for $\gamma = 0.1$ (– – – –), $\gamma = 0.3$ (———) and $\gamma = 0.4$ (– · – · –) for a system of size 60 000. The value of q is varied from -30 to -50. Figure 4(*b*) shows α_{min} versus q for $\gamma = 0.1$ (– – – –), $\gamma = 0.3$ (———) and $\gamma = 0.4$ (– · – · –) for a system of size 60 000. Here q is varied over a range of 30 to 50.

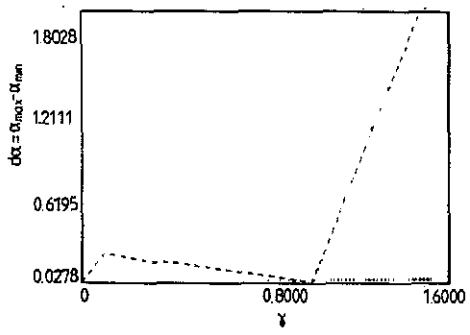

Figure 6. Plot of $d\alpha = (\alpha_{max} - \alpha_{min})$ versus γ for system size of 60 000.

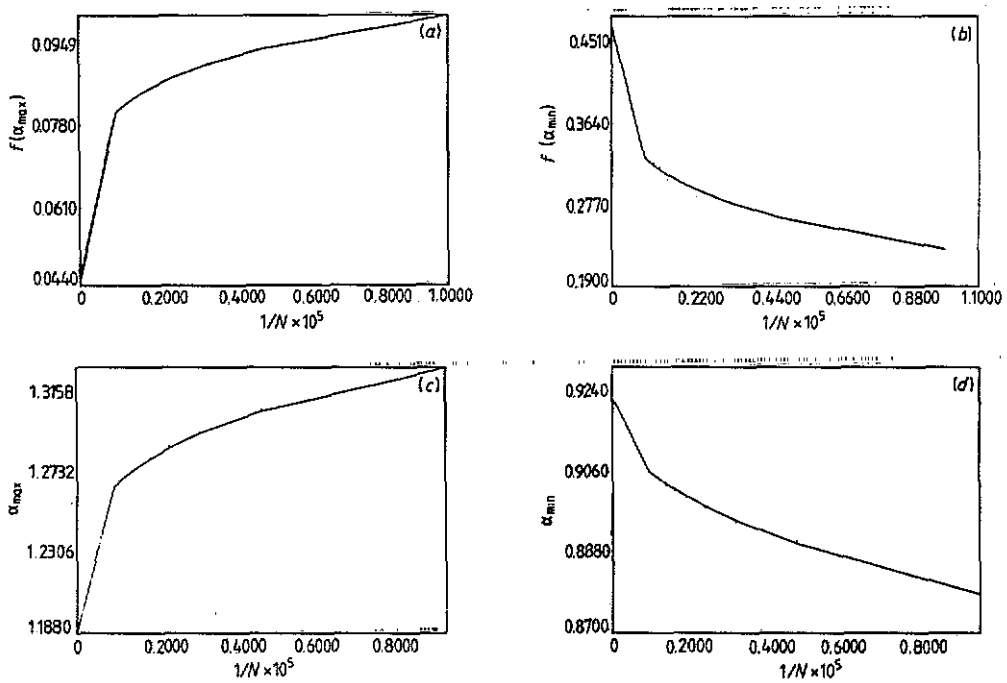

Figure 7. Plots of (*a*) $f(\alpha_{max})$ versus $1/N$ for $q = -200$, (*b*) $f(\alpha_{min})$ versus $1/N$ for $q = 200$, (*c*) α_{max} versus $1/N$ for $q = -200$ and (*d*) α_{min} versus $1/N$ for $q = 200$; here N = length/10^4.

Figure 5(*a*) shows that, as we include higher positive values of q in the definition of $Z(q)$, $f(\alpha_{min})$ decreases. Similarly figure 5(*b*) shows that inclusion of higher negative values of q leads to a decrease of $f(\alpha_{max})$. If both $f(\alpha_{max})$ and $f(\alpha_{min})$ tend to zero, as seems to be the case in these figures, this is a signature of multifractality.

Figure 6 shows the metal–insulator transition of this model of size 60 000 with respect to increasing γ values. For $\gamma = 0$, states are extended, and $\alpha_{min} = \alpha_{max} = 1$, $f(\alpha_{min}) = f(\alpha_{max}) = 1$ are expected. Here we plot $d\alpha = \alpha_{max} - \alpha_{min}$ versus γ. For an extended state $d\alpha = 0$ is expected. In the curve at $\gamma = 0$, $d\alpha \simeq 0.03$. This is because of a finite-size effect. As γ values increase, $d\alpha$ also increases. The $d\alpha$ values remain at greater than 0 but less than 0.5. At $\gamma = 1$, all states become extended again as seen by the drop in $d\alpha$

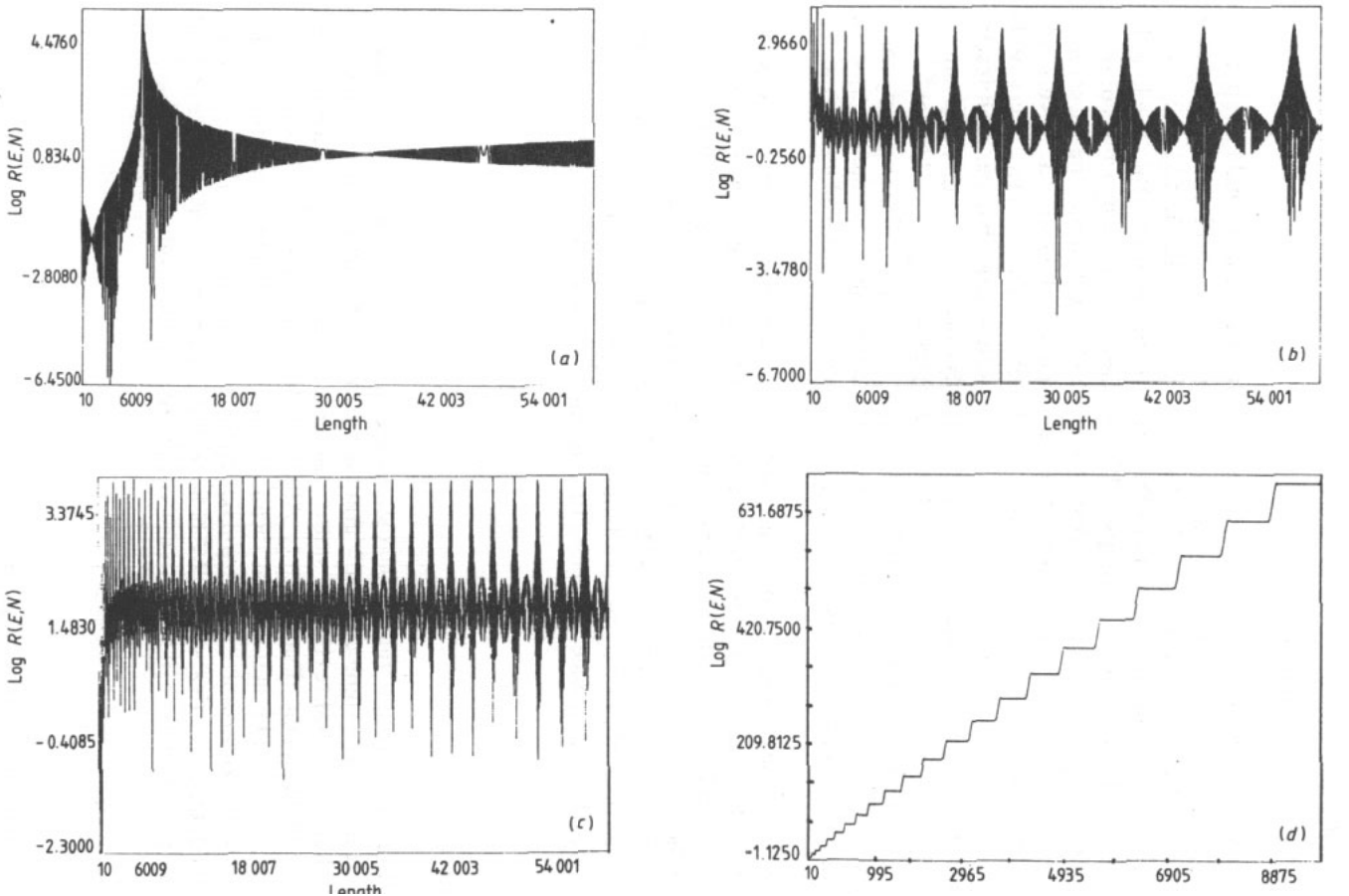

Figure 8. Plots of log $R(E, N)$ versus system size for (*a*) $\gamma = 0.1$, (*b*) $\gamma = 0.3$, (*c*) $\gamma = 0.4$ (maximum system size in (*a*)–(*c*) is 60 000), and (*d*) log $R(E, N)$ versus system size for $\gamma = 2.0$ (localized state) (maximum system size 9860).

values. But after that $d\alpha$ diverges, for *all* values of $\gamma > 1$. This is characteristic of localized states.

Next we do a finite-size scaling analysis on the multifractal properties with the following *ansatz*:

$$X_N = X_\infty + (C/N^\mu) \qquad (\mu > 0) \tag{14}$$

where X could be either α or $f(\alpha)$. Figure 7 shows the fitted curves and extrapolated values, for system size $N \to \infty$, of α_{max}, $f(\alpha_{max})$, α_{min} and $f(\alpha_{min})$ obtained in this way for $q = \pm 200$ and $\gamma = 0.3$. We have plotted the curves of α_{max}, $f(\alpha_{max})$, α_{min} and $f(\alpha_{min})$ versus $1/N$, where N denotes the length of the system scaled down by 10^4. The lengths are varied over a range 10^4 to 10^5 in steps of 10^4 and the corresponding values of these quantities noted. Then using a non-linear search method we calculated the parameters X_∞, C and the exponent μ for each of the four cases. Figure 7(*a*) shows $f(\alpha_{max})$ versus $1/N$, and the extrapolated value at $N \to \infty$ is 0.045. Figure 7(*b*) shows $f(\alpha_{min})$ versus $1/N$, and the extrapolated value at $1/N = 0$ is 0.469, so it is true that the multifractal characteristic $f(\alpha_{min})$ has decreased to a value reasonably lower than 1. Figure 7(*c*) shows α_{max} versus $1/N$; for $1/N = 0$, $\alpha_{max} = 1.188$. Figure 7(*d*) shows α_{min} versus $1/N$; at $1/N = 0$, the extrapolated value of α_{min} is 0.922, so $d\alpha = \alpha_{max} - \alpha_{min} > 0$. These clearly show the multifractal characteristics of transmittance at the critical state. All the results show that the scaling exponent behaves neither like the extended case nor like the localized case.

Figure 8 shows the evolution of resistance with system size. Resistance does not show an exponential localization (Thakur and Kumar 1990). Figure 8(*a*) shows resistance versus system size for the model potential with $\gamma = 0.1$ at the mobility edge $E_c = 1.0$. Figure 8(*b*) shows the same for $\gamma = 0.3$ at the corresponding $E_c = 0.9945$ and figure 8(*c*) shows the same for $\gamma = 0.4$ at $E_c = 0.982$. In all three cases, it is explicitly seen that the resistance does not exhibit exponential behaviour. Figure 8(*d*) shows the same for a localized state. The difference between critical-state and localized-state behaviour is clearly observed.

4. Conclusion

In conclusion we point out that critical states are seen in the vicinity of the metal–insulator transition. The significantly different behaviour of transmittance in the critical state from that of a metal (extended states) and an insulator (localized states) is well understood by a careful multifractal study. Also the behaviour of resistance distinguishes very well the critical-like states from localized states. The standard techniques like finding the inverse localization length and participation ratio do not work satisfactorily for characterization of critical states. We believe that our analysis is much more fruitful in understanding the nature of states in the vicinity of a metal–insulator transition.

References

Aoki H 1983 *J. Phys. C: Solid State Phys.* **16** L205
—— 1986 *Phys. Rev.* B **33** 7310
Aubry A and Andre G 1980 *Ann. Isr. Phys. Soc.* **3** 133
Barabási A, Szépfalusy P and Vicsek T 1991 *Physica* A **178** 17

Basu C, Mookerjee A, Sen A K and Thakur P K 1991a *J. Phys.: Condens. Matter* **3** 6041
—— 1991b *J. Phys.: Condens. Matter* **3** 9055
Chhabra A and Jensen R V 1989 *Phys. Rev. Lett.* **62** 1327
Das Sarma S, Song He and Xie X C 1990 *Phys. Rev.* B **41** 5544
Griniasty M and Fishman S 1988 *Phys. Rev. Lett.* **60** 1334
Halsey T C, Jensen M H, Kadanoff L P, Procaccia I and Shraiman B I 1986 *Phys. Rev.* A **33** 1141
Harper P G 1955 *Proc. Phys. Soc.* A **68** 874
Hiramoto H and Kohmoto M 1989 *Phys. Rev.* B **40** 8225
Kohmoto M 1983 *Phys. Rev. Lett.* **51** 1198
Kohmoto M, Kadanoff I P and Tang C 1983 *Phys. Rev. Lett.* **50** 1870
Kramer B, Ono Y and Ohtsuki T 1988 *Surf. Sci.* **196** 127
Ono Y, Ohtsuki T and Kramer B 1989 *J. Phys. Soc. Japan* **58** 1705
Ostlund S and Pandit R 1984 *Phys. Rev.* B **29** 1394
Roman E and Wiecko C 1986 *J. Phys. A: Math. Gen.* **62** 163
Schreiber M 1985a *J. Phys. C: Solid State Phys.* **18** 2493
—— 1985b *Phys. Rev.* B **31** 6146
—— 1990 *Physica* **167A** 188
Schreiber M and Grussbach H 1991 *Phys. Rev. Lett.* **67** 607
Soukoulis C M and Economou E N 1982 *Phys. Rev. Lett.* **48** 1043
—— 1989 *Phys. Rev. Lett.* **52** 565
Sutherland B and Kohmoto M 1987 *Phys. Rev.* B **36** 5877
Tang C and Kohmoto M 1986 *Phys. Rev.* B **34** 2041
Thakur P K and Kumar N N 1990 Preprint
Thouless D J 1988 *Phys. Rev. Lett.* **61** 2141